Published in *Chirality in Liquid Crystals*, H-S. Kitzerow and C. Bahr (eds), Springer (2001) p. 481.

Traveling Phase Boundaries with the Broken Symmetries of Life

P. E. Cladis
Advanced Liquid Crystal Technologies, Inc., PO Box 1314, Summit, NJ 07902 USA
Web: http://alct.com e-mail: cladis@alct.com

Abstract

Living systems are the most important and most complex of non-equilibrium liquid crystalline systems. We check an experimental minimal model for macroscopic implications of this statement. To do this, we consider "living systems" in terms of three broken symmetries: 1. liquid crystalline (broken continuous symmetry); 2. chiral (broken mirror symmetry) and 3. non-equilibrium (broken time reversal symmetry). We call these three elements the *Broken Symmetries of Life*. The surprising result is that a model system with just these three elements, also "knows time".

The minimal model system is the traveling cholesteric liquid crystal-isotropic liquid phase boundary prepared so that the length scale imposed on it by non-equilibrium driving forces is comparable to its equilibrium length, its pitch. In a pattern formation context, "knows time" means that a frequency is associated with all the patterns of this traveling interface. With the same non-equilibrium driving forces, its non-chiral analogue, the traveling nematic-isotropic liquid phase boundary, does not.

Another surprise is our minimal model's novel route to turbulence. Its non-chiral analogue prepared under identical conditions has no routes to turbulence. In contrast, as it was driven further from equilibrium, our minimal model's repertoire ranges from a cellular pattern with a single wavelength and frequency, through a wavelength doubling breathing mode, followed by a phase winding flat interface that eventually becomes turbulent.

To honor Professor Heppke's long interest in and many contributions to the study of chiral liquid crystalline materials, phase diagrams and Life, this paper is a philosophical overview of our work on the traveling cholesteric (N*)-isotropic phase boundary [1,2].

Introduction

We've heard for a long time now that living systems are the most important and most complex of known non-equilibrium liquid crystalline systems. To come up with a minimal model system to check the implications of this statement, we select three characteristics of living systems. We call them the Broken Symmetries of Life [2].

Broken Continuous Symmetry

The first is that living systems are liquid crystalline. Liquid crystals are orientationally ordered molecular liquids. When a molecular liquid is in the isotropic liquid state (which models the primordial soup), it has neither translational nor orientational order. At the phase transition to the nematic state, the most basic liquid crystal transition, the system selects a special direction for long range orientational order. This direction is called the director and denoted by a unit vector, **n**. By selecting a special direction, the nematic breaks the continuous rotational symmetry of the isotropic liquid. A phase boundary intervenes between the nematic and the isotropic liquid when they coexist.

Broken Mirror Symmetry

The second living system feature we select is that they are chiral. We take this to mean broken mirror symmetry. In liquid crystals, chirality is expressed as a macroscopic helix with a pitch, p_o. In cholesteric liquid crystals, $1500\text{Å} < p_o < \infty$, and $\mathbf{q_o}$, its wavevector (wavenumber $q_o=2\pi/p_o$), is perpendicular to **n**, the direction of orientational order. The existence of this intrinsic equilibrium length has several implications of which we mention two particularly insightful ones [1,2].

The first is that in a diffusive process e.g. orientational diffusion in liquid crystals, characterized by a diffusion constant, $D_o \equiv K_2/\gamma_1$, where K_2 is the twist elastic constant and γ_1 the rotational viscous coefficient. In a system with an equilibrium length scale, q_o, a characteristic frequency $\omega_{el} = D_o q_o^2$ can be defined. By comparing the magnitude of this frequency with experimental observations, we can assess the importance of the various diffusion processes at work in a given situation. If the observed ω is such that $\omega/\omega_{el} \sim O(1)$, this tells us that the most important dissipative process involved at the traveling cholesteric-isotropic phase boundary is orientational diffusion as indeed it turns out to be for patterns closer to equilibrium [1,2].

The second is that a mirror transformation such as $z \rightarrow -z$ results in $q_o \rightarrow - q_o$: in a mirror, a right hand is a left hand. As pointed out by Brand and Pleiner [3], the handedness of q_o allows terms in the dynamic equations coupling q_o to gradients of a scalar such as $\tilde{\mathbf{N}}T$, a temperature gradient, or $\tilde{\mathbf{N}}c_\infty$, gradients in concentration.

Broken Time Reversal Symmetry

A third feature of living systems is that they are a consequence of many diffusive processes that can only be sustained by continuous energy input. Living systems are far from equilibrium where no energy input is required. They are non-equilibrium systems characterized by broken time reversal symmetry.

How do we model these three broken symmetries of life before being carried off to be burned at the stake?

A Minimal Model System

The first Broken Symmetry of Life, we identified with a liquid crystal-isotropic liquid transition. Something (i.e the liquid crystal order parameter) emerges from nothing, the primordial soup.

To model the second element of Life's Broken Symmetries, we chose cholesteric liquid crystals (N*) as they are chiral liquid crystals.. We made C15-8CB cholesteric-nematic mixtures where the concentration, c_∞, of C15 in 8CB lowered the cholesteric-isotropic transition temperature by: $T_{ChI}(^oC) = 40.36 - 0.22c_\infty(\%)$. The pitch decreased with c_∞ as $q_o(\mu m^{-1}) = 0.02c_\infty(\%)$: the more C15, the lower the transition temperature and the tighter the pitch and vice versa. The sample cell was the usual two parallel glass plates assembly with separation $d \approx p_o \approx 38\mu m$. The glass plates were prepared so that **n** was uniform and in the plane of the glass.

To put the N*-iso transition line into a non-equilibrium state, we force it to move at a velocity, **v**, through a temperature gradient **G||v.** The temperatures at the hot and cold contacts are chosen so that T_{ChI} is in the middle of the field of view of a polarizing microscope (Fig. 1). We force v on the interface by displacing the sample at speed, -v, towards the cold contact. As the transition temperature is fixed in the lab frame, displacing the sample towards colder temperatures forces the N*-iso. phase boundary to move towards the hot contact to maintain

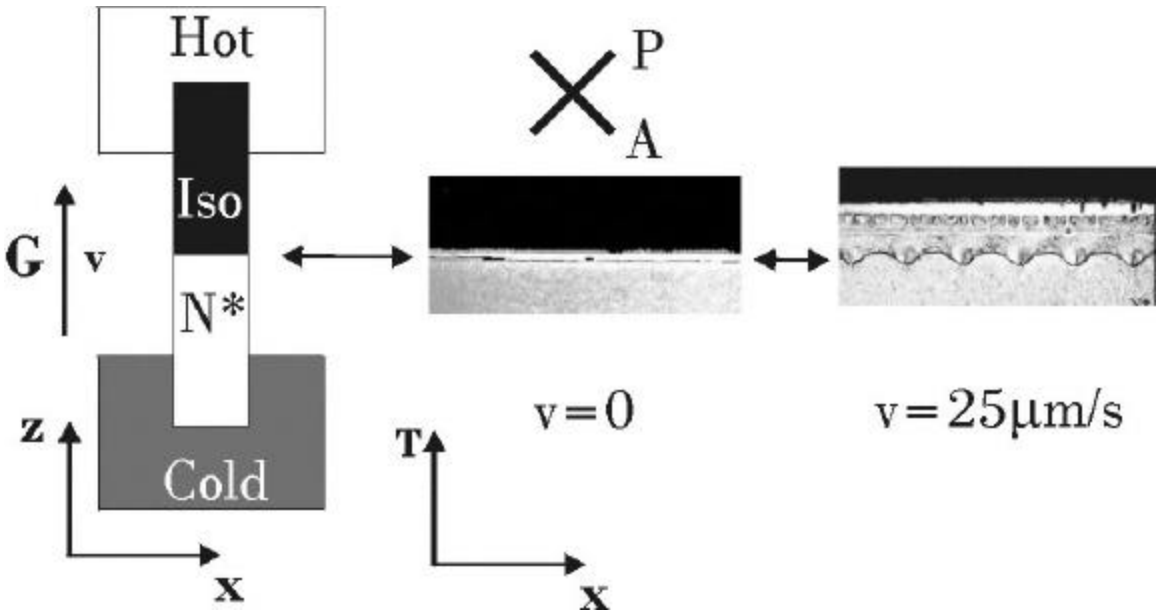

Figure 1. The sample is loaded with **n** at the surfaces ' **n||G,** the temperature gradient**.** *Left*: Experimental set-up for directional solidification. **G||v,** the velocity of the N*-iso. phase boundary as the sample is displaced from the hot contact to the cold one at speed, -v. *Center*: The flat interface when $v<v_c$ =19μm/s. As z=0 at the interface and T(K)=Gz, the picture dimensions are 250μm×0.25K. *Right*: 510mm×0.3K picture of the modulated interface. Its wavelength, λ=104μm when v=25μm/s $>v_c$. Those parts of the interface towards higher temperatures (*tips*) are less rich in C15 therefore have a larger pitch than those at lower temperatures (*grooves)*. The two headed arrows highlight the transition line. Note increase in the N*-isotropic meniscus in the moving sample.

T_{ChI}.

This is a well-known technique called Directional Solidification. It was invented by Jackson and Hunt to advance industrial crystal growth processes [4]. Improvements in our set-up compared to their original one include several computer controlled stepping motors and image processing software.

Pattern Formation in Liquid Crystals

While pattern formation, epitomized by beautiful snowflakes, was first liberated from theology by Kepler in 1611, it is only relatively recently some progress has been made in its scientific investigation [5]. Pattern formation refers to spatial structures, usually characterized by a band of wavelengths, that replace a uniform state above a critical distance from equilibrium. Patterns are non-equilibrium structures resulting from several dissipative processes characterized by diffusion constants. They are quantified by their wave-vector, **q**, and their frequency, ω.

A phase boundary forced to travel by mechanical displacement at speed, -v, in a temperature gradient, **G**, is a model pattern forming system (Fig. 1). It has the advantage that both **G** and **v** can be well-controlled. Because liquid crystals are a strategic component of the semiconductor industry, they are well-characterized. Consequently, reliable information can be obtained from the various patterns exhibited by traveling liquid crystal phase boundaries.

Another important strength of cholesteric and nematic liquid crystals in this context is that they are 3D liquids. As a result, transitions from equilibrium to full-scale turbulence can gracefully evolve so can be followed in the lab frame. All length and time scales do not suddenly appear at one transition, or bifurcation, as they do at e.g the traveling TGB_A-smectic A phase boundary [6].

Constitutional Supercooling

What are the processes at work to make a pattern in directional solidification? As the interface advances, it expels impurities into the isotropic liquid. The impurity excess at the interface follows linear diffusion to exponentially decay from a maximum at the interface (c_I) to c_∞ far from the interface: $c(z) = c_\infty + \Delta c \bullet \exp(-z/l_D)$. $\Delta c = c_I - c_\infty$. The characteristic length for this decay is the dynamic diffusion length, $l_D = D_I/v \sim 2\mu m$ when $v = 20\mu m/s$. D_I is the impurity diffusion constant, $D_I = 2\times10^{-7} cm^2/s$ [7]. Here the impurity is C15, the chiral agent. In liquid crystals, setting up a steady state concentration gradient in front of the moving interface is relatively fast with a characteristic time, $\tau_D = D_I/v^2 \sim 0.2s$ when $v \sim v_c = 19\mu m/s$. Impurity diffusion is the only destabilizing non-equilibrium force in this system. Above a critical speed, v_c, the destabilizing force of the impurity gradient overcomes the stabilizing forces of the temperature gradient and the elastic forces, so that a pattern characterized by both a $q < q_o$ and frequency, $\omega/2\pi$, form at the interface (Fig. 1 right).

The classic argument for why a flat traveling phase boundary becomes unstable to a pattern in directional solidification is called *constitutional supercooling* [9]. The argument is easily

understood when one keeps in mind that a temperature gradient maps temperature onto space: T (K) =Gz (Fig. 1).

A pertubation of the interface into the hotter region puts it in contact with isotropic liquid at temperature T(z) and concentration c(z). If the concentration gradient does not fall steeper than the equilibrium c_∞-T_{ChI} slope, this isotropic liquid is warmer than the interface so the bump melts stabilizing the flat interface. As v increases, the dynamic diffusion length, l_D, decreases so that at v_c the concentration gradient is steeper than the equilibrium c_∞-T_{ChI} slope. In this case, a perturbation now puts the interface in contact with isotropic liquid that is purer than it's supposed to be i.e. the isotropic liquid is at a lower temperature than dictated by c_∞-T_{ChI}. It is locally supercooled because its impurity level is too small for its temperature. Thus the name *constitutional supercooling*. This is an unstable situation so the bump on the interface grows into the isotropic liquid nucleating a pattern called a cellular pattern (Fig. 1 right).

While constitutional supercooling explains why one bump grows, it does not account for a line of bumps with wavenumber, q. The outstanding question of pattern formation is still: Where does q come from? Nevertheless, at the traveling nematic-isotropic phase boundary and the traveling N*-iso. phase boundary, the cellular pattern has a length scale - not a band - that is a result of non-equilibrium forces acting on the system.

The Traveling Cholesteric-Isotropic Interface "Knows" Time

The surprising result is that our liquid crystal model system with just these three broken symmetries of life "knows" time, another feature of living systems. It does not learn about time after it has been pushed far from equilibrium and is close to turbulence. It knows time as soon as the non-equilibrium driving force is strong enough to enforce a pattern. Even its first pattern is characterized by a frequency, ω. When v $\rightarrow$ 0, the interface reverts back to its featureless dead state: q = 0 and ω = 0.

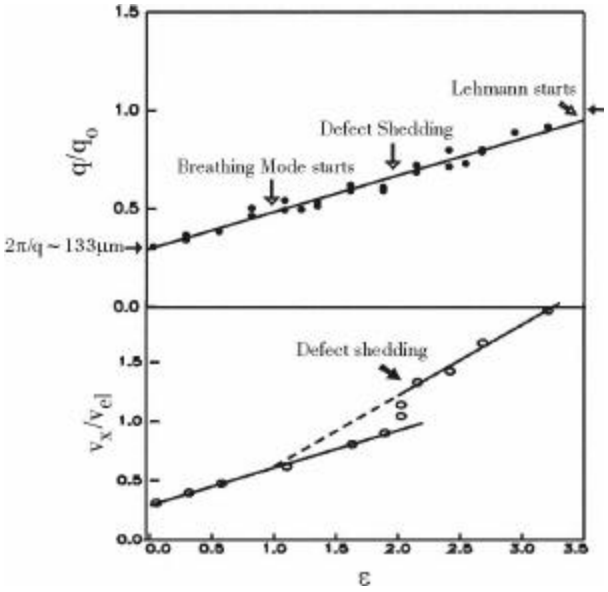

Figure 2. Pattern wavenumber, q, scaled by q_o and speed parallel to the interface, v_x, by v_{el}, as a function of the control parameter, $\varepsilon \equiv (v-v_c)/v_c$.

To recognize that there is a time scale at the pattern onset is a bit subtle (Fig. 1). The evidence is that the pattern travels parallel to the interface at speed v_x as soon as $q \neq 0$. At the pattern onset, v_x is small (~1μm/s) so its movement is not obvious to the impatient eye. With increasing distance from equilibrium, measured by a control parameter called $\varepsilon \equiv (v-v_c)/v_c$, v_x increases (Fig. 2) so that its motion becomes more obvious.

Despite all the drama at the cellular interface when $\varepsilon < 3.5$ (Fig. 2), q is linear in ε: $q/q_o = 0.19\varepsilon + 0.29$, independent of the dynamics. On the other hand, v_x has two responses. When $\varepsilon < 2$, $v_x/v_{el} = 0.32\varepsilon + 0.3$: the cholesteric texture left by the traveling phase boundary is unstructured and there are no director relaxation processes observed when $v \rightarrow 0$. When $\varepsilon > 2$, $v_x/v_{el} = 0.60\varepsilon + 0.03$: v_x increases twice as fast as when $\varepsilon < 2$. The texture left behind the traveling interface is a uniform array of line defects (one line per cell) that slowly disappears by defect coarsening when $v \rightarrow 0$ [1]. We note that taking into account the scatter in the data, the intercept of v_x's $\varepsilon > 2$ line is zero and that it intersects its $\varepsilon < 2$ line at $\varepsilon \approx 1$ where the breathing mode starts.

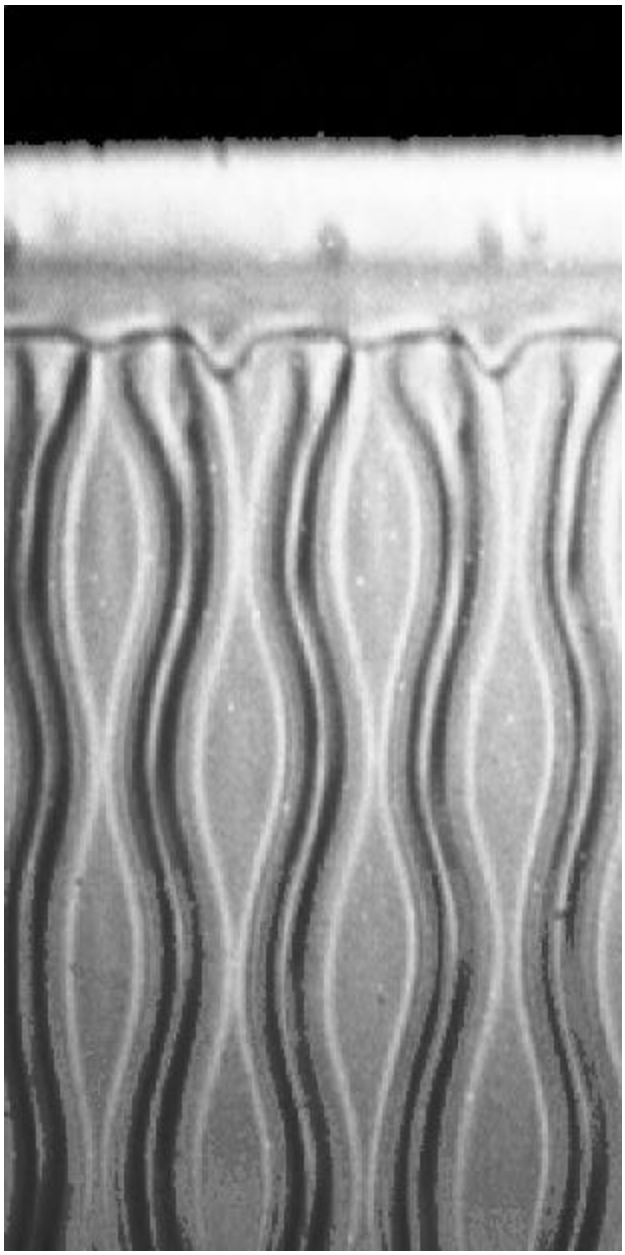

Figure 3. Snapshot of the breathing mode decorated by defect lines.

Breathing Mode

When $0.5q_o < q < q_p$, we observed a breathing mode (Figs. 2, 3). It starts at ε=1. In addition to traveling, the pattern also oscillates with a frequency, ω. In one half cycle of ω, alternate *grooves* grow while in the other half cycle, they shrink, doubling the pattern wavelength (Fig. 3). For the breathing mode, $\omega/\omega_{el} = -0.23 + 1.13q/2q_o$. The breathing mode is nonlinear and nondispersive [1].

At $\varepsilon = 2$, the interface starts to shed defects and v_x doubles (Fig. 2). Fig. 3 is a snapshot after the start of defect shedding. The memory of the position of the defect line at the interface at the time it was shed is topologically trapped thus dramatizing the breathing mode for Fig. 3.

We interpret the appearance of a frequency in the cellular regime of the traveling N*-iso. phase boundary, as resulting from a competition between the non-equilibrium length scale, q and the equilibrium length scale, q_o.

Diffusion Processes

1. *Orientational Diffusion:* As already mentioned, the liquid crystal's orientational diffusion process is the dominant process at work in the cellular regime where $q \neq 0$ and $\omega \neq 0$. The diffusion constant characterizing this process is $D_o = 8\times10^{-7}cm^2/s$ [9]. By scaling q with $q_o = 2\pi/38\mu m$, v_x with $v_{el} = D_o/p_o = 2.1\mu m/s$ and ω by ω_{el}, we saw that v_x/v_{el}, q/q_o and ω/ω_{el} are O(1).
2. *Thermal Diffusion:* The characteristic length for this process is the thermal length, defined by $l_T \equiv \Delta T_c/G$ where ΔT_c is the width of the two phase region of the cholesteric-isotropic transition. As G increases l_T decreases. For the concentration of C15 used in this experiment, $\Delta T_c = 0.1K$ giving an $l_T \approx 133\mu m$. This is about 3.5 times p_o and close to the pattern wavelength at onset (Fig. 2).
3. *Impurity Diffusion:* This process is characterized by the dynamic diffusion length, $l_D = D_I/v$. As v increases, l_D becomes even smaller. When the Lehmann effect appears (Fig. 4), $l_D \approx 0.1\ \mu m$ making impurity diffusion the dominant effect controlling the coupling between q_o and gradients in a scalar field.

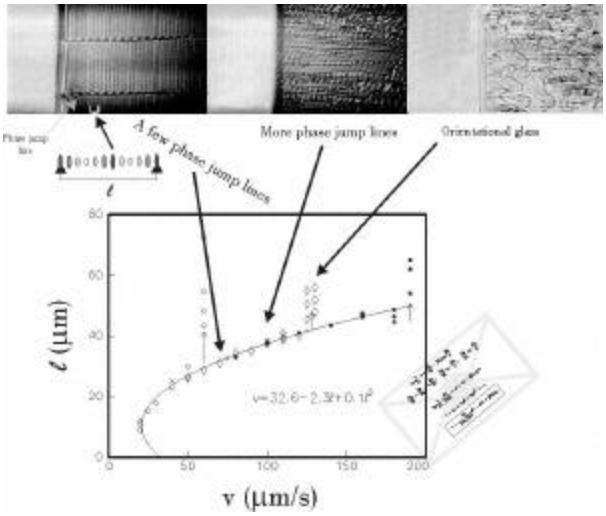

Figure 3. When G is large, the interface is flat, q = 0, (top left snapshot) but the director winds at the interface , $\omega \neq 0$, leaving behind in the cholesteric state a striped pattern of wavelength, *l*. The phase winding is coherent (ϕ_o = constant) along the interface between phase jump lines where ϕ_o jumps by π or 2π. The different symbols in the graph are for different values of G. For a given G, the Lehmann effect starts at a minimum v and there are a few phase jumps lines. As v increases, phase jump lines become more numerous. Finally, at a maximum v for a given G, they are so numerous, *l* can no longer be measured. We identify all points not on the universal parabola, as being in the orientational glass state.

Lehmann Effect

Driving the system even further from equilibrium, resulted in a pattern appearing behind the flat interface (Fig. 4). In this second regime, q = 0 but $\omega \neq 0$. Here the patterns are generated by the non-equilibrium phase winding of **n** at the interface.

Phase winding in cholesterics was first observed by Otto Lehmann, the physicist father of liquid crystals, and is known as the Lehmann effect. Brand and Pleiner [3] were the first to account for the Lehmann effect with a straight forward symmetry argument that can be used to extract a Lehmann coefficient [2].

Symmetry Argument for the Lehmann Effect

For a helix with q_o oriented along **z, n** = (cosϕ, sinϕ, 0) with $\phi = q_o z + \phi_o$. ϕ is the director phase relative to a fixed direction in the xy-plane and ϕ_o is an arbitrary constant. The operation $z \rightarrow -z$ changes $q_o \rightarrow -q_o$: the right handed helix becomes a left handed one.

This symmetry allows terms in the dynamic equation [3] coupling q_o to gradients of a scalar i.e. terms such as $d\phi/dt \sim q_o\, dT/dz \sim \nu_T / \ell_T$ and $d\phi/dt \sim q_o\, dc/dz \sim \nu_c / \ell_D$. ν_T and ν_c are the Lehmann coefficients for the coupling of q_o to temperature and concentration gradients respectively. $d\phi/dt \neq 0$ means that **n** rotates in time at fixed z in the lab frame in a process we called phase winding. As $\ell_D << \ell_T$, it is the dominant effect to account for phase winding in (Fig. 4). Putting in the constants, we have: $\gamma_1\, d\phi/dt = \nu_c / \ell_D$.

In a "back of the envelope" calculation (Fig. 4), we expand this last to relate the observed wavelength behind the interface, ℓ, to the interface speed, v, and hence deduce the Lehmann coefficient [2].

With increasing v, the spatial correlations in phase winding became shorter and shorter as the system is driven still further from equilibrium (Fig. 4). Eventually a spatially and temporally disordered state is observed. We call this last state, the third regime, an orientational glass. In this regime there are many q's and many ω's.

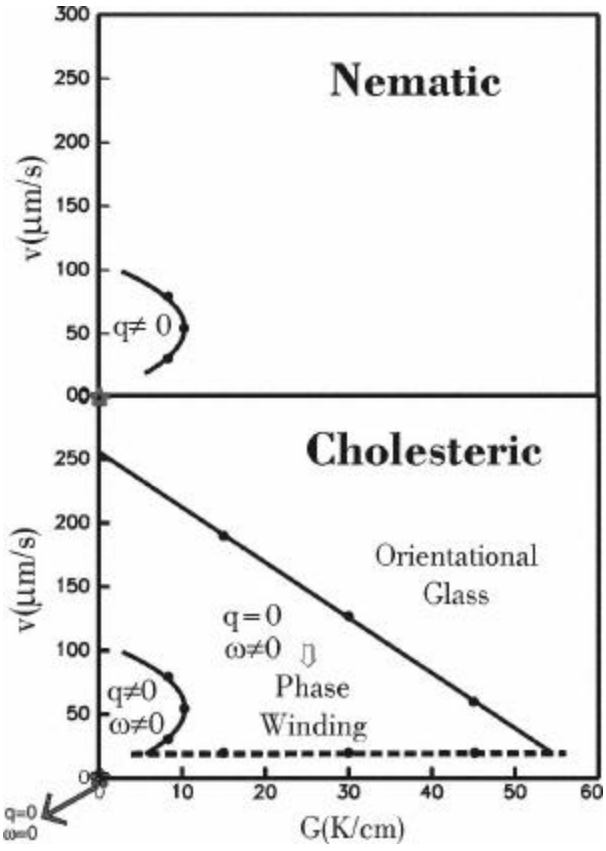

Fig. 5. Comparison between patterns with (bottom) and without (top) chirality.

Phase Diagram

The crucial role played by chirality in these studies is highlighted with the type of phase diagram (Fig. 5) much beloved by Professor Heppke. The two control parameters for these experiments are v and G, both of which can be precisely controlled. Equilibrium is when v and G are zero. As v and G increase, the system moves further from equilibrium.

The phase diagram for the traveling cholesteric-isotropic interface has three regimes (Fig. 5 bottom). In the first regime, where cellular patterns are observed, $q \neq 0$ and $\omega \neq 0$, the dominant diffusion process is orientational diffusion. The breathing mode is observed in this regime. In the

second regime, where phase winding is observed, $q = 0$ and $\omega \neq 0$, the dominant process is impurity diffusion. G is sufficiently large that the interface is flat but there is a pattern left behind the interface. The last regime is the orientational glass state where the cholesteric is both spatially and temporally disordered.

The cholesteric phase diagram can be compared to what is observed in a nematic liquid crystal under the same non-equilibrium conditions (Fig. 5 top). In the traveling nematic-isotropic interface, only the reentrant cellular regime near equilibrium is observed. And in this regime, there is no frequency associated with the patterns: $q \neq 0$ but $\omega = 0$. At higher speeds and larger temperature gradients, the interface is only flat: $q = 0$ and $\omega = 0$.

Conclusions

The existence of an intrinsic length, p_o, in cholesteric liquid crystals, implies a frequency for its response to perturbations in its structure. When $q \sim q_o$, the dominant diffusive process is orientational diffusion. In this cellular regime, the patterns have both $q \neq 0$ and $\omega \neq 0$. Further from equilibrium, the dominant diffusive process is impurity diffusion triggered by the concentration gradient in advance of the moving interface. While the interface is flat, the director winds at the interface leaving behind a striped pattern: $q = 0$ and $\omega \neq 0$. In this regime dominated by impurity diffusion, phase winding is coherent between phase jump lines where ϕ_o jumps by π or 2π. As the interface travels faster in the temperature gradient, the distance between phase jump lines decreases as they become more numerous. Eventually, there are so many phase jump lines, a wavelength can no longer be measured and the orientational glass state takes over. In the orientation glass state, the texture behind the interface is disordered in both space (many q's) and time (many ω's).

The macroscopic implication of the Broken Symmetries of Life shown by the minimal model is profound: because living systems necessarily know time, they also have access to turbulence.

Finally, we conclude that with his interest in chirality in liquid crystals for many years now, an interest we have shared, Professor Gerd Heppke has demonstrated his perspicacity and good taste in scientific problems. May you have many more years of happy experiences offered by the ineluctable pleasures of chirality - and the Broken Symmetries of Life - particularly broken time reversal symmetry.

Χρόνια Πολλα'!

References

1. P. E. Cladis, J. T. Gleeson, P. L. Finn and H. R. Brand, *Breathing Mode in a Pattern Forming System with Two Competing Lengths*, Phys. Rev. Lett. **67**, 3239 (1991); P. E. Cladis, *Pattern Formation at the Cholesteric-Isotropic Interface* in Pattern Formation in Complex Dissipative Systems, S. Kai (ed), World Scientific, Singapoere (1992) p. 3.
2. H. R. Brand and P. E. Cladis, *Nonequilibrium Phase Winding and its Breakdown at a Chiral Interface* Phys. Rev. Lett., **72**, 104 (1994); P. E. Cladis and H. R. Brand, *Nonequilibrium Phase Winding and its Breakdown at a Chiral Interface* in Spatio-Temporal Patterns in Nonequilibrium Complex Systems, P. E. Cladis and P. Palffy-Muhoray (eds), Addison Wesley, Reading, MA (1995) p. 123.
3. H. R. Brand and H. Pleiner, *New Theoretical Results for the Lehmann Effect in Cholesteric Liquid Crystals*, Phys. Rev. **A37**, R2736 (1988).
4. K. A. Jackson and J. D. Hunt, *Transparent Compounds that Freeze like Metals*, Acta Metall. **13**, 1212 (1965).
5. J. S. Langer, Science, 243, 1150 (1989).
6. P. E. Cladis, A. J. Slaney, J. W. Goodby and H. R. Brand, *Pattern Formation at the Traveling Liquid Crystal Twist Grain Boundary Smectic A Interface*, Phys. Rev. Lett. **72**, 226 (1994).
7. M. Hara, H. Takezoe and A. Fukuda, Jpn. J. Appl. Phys. **25,** 1756 (1986).
8. J. W. Rutter and B. Chalmers, Can. J. Phys., **31**, 15 (1953); W. A. Tiller, K. A. Jackson, J. W. Rutter and B. Chalmers, Acta. Metall. **1,** 428 (1953).
9. $D_o = K_2/\gamma_1$ where K_2 is the twist elastic constant measured for 8CB by M. J. Bradshaw, E. P. Raynes, J. D. Bunning and T. E. Faber, J. Phys. (Paris), **46**, 1513 (1985) and $\gamma_1 = 0.25 dyn/cm^2/s$ by H. Kneppe, F. Schneider and N. K. Sharma, J. Chem. Phys., **77**, 3203 (1982).